EXPERIMENTAL DETERMINATION OF THERMAL CONDUCTIVITY IN PARTICLE BEDS

JIRI DOBIAS[1], JAKUB HLOSTA[1], JIRI ROZBROJ[1], DAVID ZUROVEC[1], JAN DIVIS[1], LEO KASPERCIK[1], KAMILA POKORNA[1], JIRI ZEGZULKA[1], JIRI NEUWIRTH[2], JAN NECAS[1]

[1]VSB-Technical University of Ostrava, Faculty of Mining and Geology, Department of Mining Engineering and Safety, 17. listopadu 15/2172, 708 00, Ostrava-Poruba, Czech Republic

[2]WISTA s.r.o., Dlouhe dily 414, 763 02, Zlin-Louky, Czech Republic

DOI: 10.17973/MMSJ.2026_11_2026092

e-mail: jakub.hlosta@vsb.cz

ABSTRACT

Thermal properties are key parameters in many industrial processes involving particulate materials, yet their determination remains challenging due to the heterogeneous nature of bulk solids. This study presents an experimental method and laboratory device for evaluating thermal conductivity under controlled heating conditions. The setup is based on unidirectional heat conduction and determines relative thermal conductivity from temperature gradients measured within a cylindrical chamber. Experiments with glass spheres (1.5–5 mm diameter) showed that effective thermal conductivity decreases as particle size increases, primarily due to changes in packing density and inter-particle contact resistance. The observed trend was confirmed using a TEMPOS Thermal Properties Analyzer. Although absolute conductivity differences were small, the method consistently captured relative variations and proved suitable for CFD–DEM model calibration. The approach is applicable to particles from a few millimetres to several tens of millimetres and is relevant to clinker cooling, bulk material handling, and thermal energy storage.

KEYWORDS

Thermal conductivity, Unidirectional heat conduction, Granular media, Particle size, Experimental method

1 INTRODUCTION

Thermal conductivity ($W \cdot m^{-1} \cdot K^{-1}$) is a fundamental physical property essential for heat-transfer calculations [Shapiro 2004; Hlosta 2017]. Measuring temperature gradients in a material provides insight into its ability to conduct heat and is particularly important for particulate systems, where heterogeneous packing and contact resistance strongly affect heat transport.

Thermal characteristics of particulate materials play a crucial role in several energy-intensive industries, including cement production, power-plant ash handling, and food processing. Inefficient thermal management can lead to process instability, excessive energy consumption, higher costs, and negative environmental impacts. In cement manufacturing, for example, clinker production at ~1450 °C requires substantial fuel input, and thermal efficiency directly influences operating costs [Park 2023; Liu 2014; Verma 2020; Costa 2023]. Effective clinker cooling from ~1350 °C to below 100 °C is essential, yet many plants struggle to cool below 250 °C due to system limitations [Oyepata 2021 ; Collier 2016]. Improved thermal control reduces fuel use and lowers greenhouse-gas emissions [Moses, 2023]. Similar benefits apply in the food industry, where thermal properties determine heat-transfer efficiency during operations such as drying, frying, or pasteurization [Carson 2015; Cahyaningrum 2024].

As industrial systems become increasingly complex and advanced modelling methods, especially CFD and DEM are used to optimize thermal processes such as clinker cooling, fluidized handling of solids, or bulk heat-storage beds [Oyepata 2021; Hlosta 2018a; Hlosta 2018b]. Accurate input data for such models require reliable measurement of thermal conductivity in particulate materials.

A wide range of techniques exists for determining thermal conductivity, including steady-state guarded-hot-plate systems [Mirkovic-Marjanovic 2022; Stepanic 2019], parallel-conductance methods for anisotropic materials [Cheng 2017], and several transient approaches such as laser flash or the 3-omega method [Chalise 2023; Gu 2009; Cahill 2004]. Further options include hot-wire and hot-ball techniques [Lee 2006; Salim 2022]. However, most commercially available devices rely on cylindrical heat propagation and are optimized for liquids or compact solids, not for coarse granular materials with variable morphology, high porosity, and limited sensor–particle contact. As a result, existing techniques typically provide absolute values with limited relevance to large-scale particulate beds.

Despite extensive development of thermal-conductivity measurement techniques, there is no simple, robust, and scalable method tailored specifically to coarse particulate materials (mm–cm scale) that enables reliable comparison

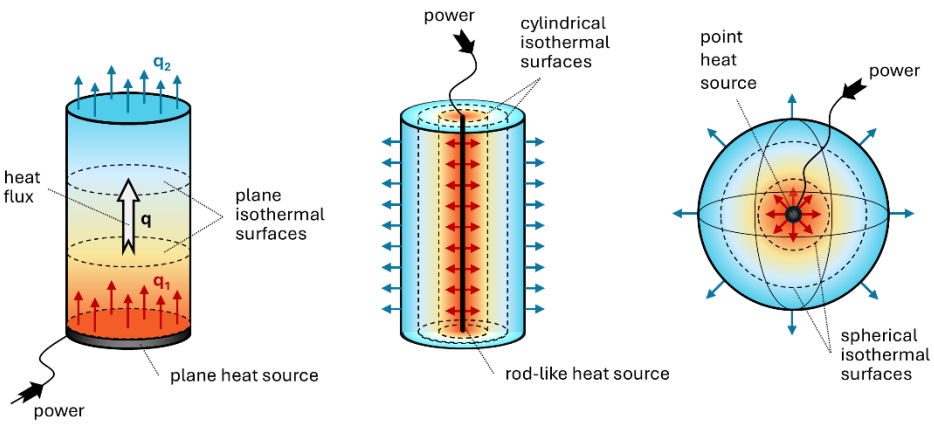


Figure 1. Different types of isothermal surfaces

between samples and supports calibration of CFD-DEM heat-transfer models. Current methods are either optimized for fine powders or require ideal contact conditions that are difficult to achieve in granular beds.
This work introduces a new experimental method and laboratory device based on unidirectional heat conduction for comparing the relative thermal behaviour of particulate materials under nominally similar heating conditions. The method is used to investigate the influence of particle
size on the temperature gradients within a granular bed and to assess its potential for providing comparative data for future CFD–DEM simulations of heat transfer in granular systems. Heat transfer in granular beds remains relatively understudied compared with other bulk-solid properties, making it an important phenomenon that deserves further investigation.

2 METHOD DETAILS

The principle underlying the measurement of thermal conductivity in granular media, as employed in the proposed method, requires the establishment of an isothermal field of planar, cylindrical, or spherical geometry, as depicted in Fig. 1. The design of the method and the measuring apparatus is based on Fourier's law, which governs unidirectional heat flux within a body. In practice, one end of a material column is maintained at an elevated temperature, and the resulting temperature gradient is recorded at predetermined distances from the heat source once a steady-state thermal regime has been reached.
This method is intended for measuring the thermal properties of particulate materials and comparing them either across materials with different bulk characteristics or against selected reference standards. A specified amount of material is placed in a vertically oriented cylindrical chamber. The side walls of the chamber are insulated, the bottom is heated using an electric hot plate, and the top is open to the surrounding environment at a constant temperature. Thermometers are positioned along the vertical axis of the chamber at equal intervals to record the temperature profile of the sample.

2.1 Method description

If we assume proper insulation of the outer wall comprising the thermal resistance of the insulation material, the wall itself, and a portion of the sample we can consider the system as a basic cylindrical field with unidirectional heat flow, as shown in Fig. 1. Heat flux q1 is supplied to the bottom plate of the cylinder, while heat flux q2 escapes through the top plate and dissipates into the surrounding environment. In steady-state conditions, this situation can be described by the well-known Fourier's law of unidirectional heat conduction:

$$q = -\lambda \cdot \frac{dT}{dx} \tag{1}$$

where q is the heat-flux density, λ is the thermal conductivity, and dT/dx is the temperature gradient in the x direction.
The thermal conductivity of the bulk solid can then be determined using the equation:

$$\lambda = -q \cdot \frac{\Delta x}{\Delta T} \tag{2}$$

where Δx is the height of the material corresponding to the measured temperature difference ΔT.
Since the objective is to compare different samples under nominally identical heating conditions, the parameter Δx can be omitted because it remains constant for all experiments. Likewise, the heat-flux density q may be omitted under the assumption of constant heating power and fixed heat-flow direction; the negative sign in Fourier's law is irrelevant for comparative purposes. With these assumptions, Equation (2) can be simplified as follows:

$$\lambda \sim \frac{1}{\Delta T} \tag{3}$$

Thus, the thermal conductivity becomes inversely proportional to the measured temperature difference, provided that the heat flux through the evaluated sections is sufficiently similar between experiments. Consequently, differences in temperature gradients between samples may indicate differences in their relative effective thermal conductivity: a higher temperature difference indicates a lower thermal conductivity relative to the reference sample and vice versa, provided that the heat flux through the evaluated sections is comparable. The assumption of comparable heat flux represents an approximation rather than an experimentally verified condition.

2.2 Device description

A schematic representation and a photograph of the experimental device are shown in Fig. 2. The apparatus consists of a refractory cylinder (Fig.2 pos. 1) with an internal diameter of 200 mm forming the main chamber (2). The cylinder is mounted on a supporting frame (Fig.2 pos. 3) and insulated with a 30 mm layer of mineral wool insulation (Fig.2 pos. 4) with declared thermal resistance 0.4 m·K/W at 200 °C. An electric hot plate (Fig.2 pos. 5) with a maximum rated power of 1500 W is positioned at the bottom of the chamber. The joint between the hot plate and the cylinder is sealed with ceramic fibre rope (Fig.2 pos. 6).

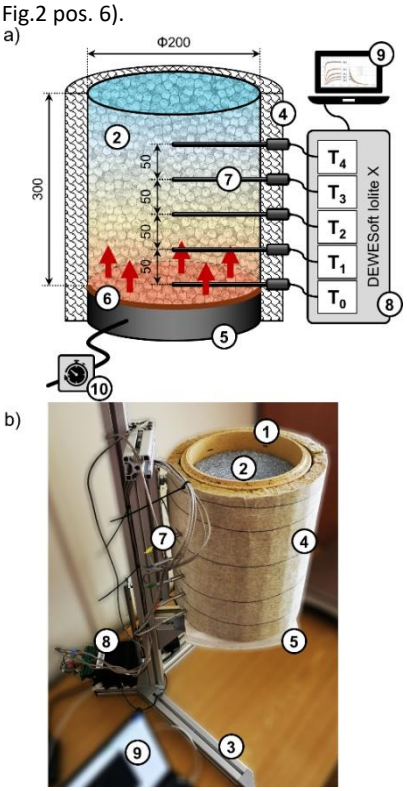


Figure 2. Schematic depiction of the experimental device, (1) refractory cylinder; (2) chamber; (3) frame; (4) insulation; (5) hot plate; (6) chamber perimeter sealing; (7) temperature sensor; (8) DeweSoft data acquisition module Iolite X; (9) laptop; (10) digital timer socket

Five PT100 needle temperature sensors (Fig.2 pos. 7) are installed along the height of the chamber, with the first placed 5 mm above the hot plate and the remaining sensors spaced at 50 mm intervals. The top of the chamber is open to the ambient environment. The material is filled to a height of 300 mm, resulting in a total chamber volume of 9.4 dm^3. An

additional thermometer is positioned outside the chamber to monitor the surrounding temperature.
All temperature sensors are connected to a DeweSoft® data acquisition module (Fig.2 pos. 8), which is linked to a laptop (Fig.2 pos. 9) for data recording. The hot plate is operated through a digital timer socket (Fig.2 pos. 10) that controls the heating and cooling cycles.

2.3 *Measurement process*

The experimental procedure begins by filling the chamber with a specified amount of the sample. It must be ensured that all thermometers are positioned vertically and at the correct depths within the material. The data acquisition system is then connected to the sensors and to a computer running the measurement software. After filling, sufficient time is allowed for all sensors to equilibrate to the same initial temperature. This initial temperature is recorded as the starting reference, and only the subsequent temperature difference relative to this value is monitored (T1-T4 = 0 K at start of data recording). The hot plate is subsequently switched on, initiating the heating phase. Heating continues until the temperatures recorded by all sensors become sufficiently stable and no longer increase, indicating that the system has reached thermal equilibrium.

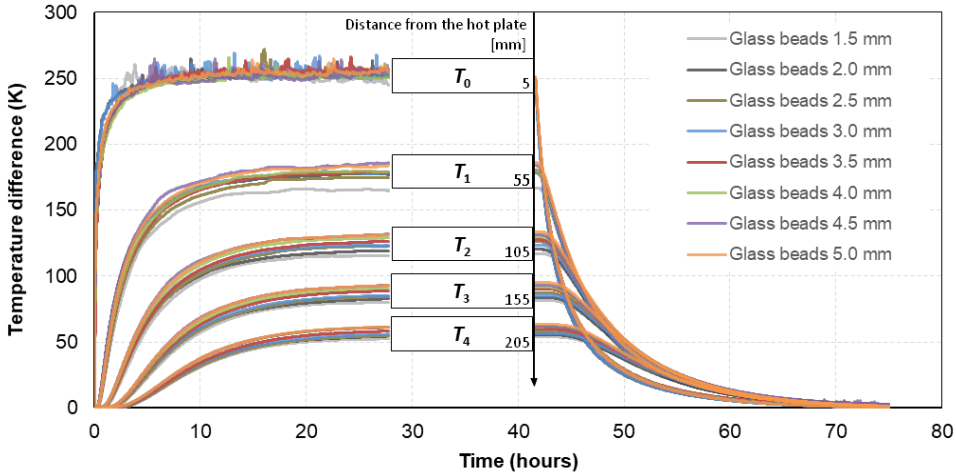


Figure 3. Data plots obtained from measurements of various bead diameter samples

The heating power is then turned off, and the sample enters the cooling phase. Cooling is complete when all sensors again record a uniform and steady temperature. Recorded data is saved, chamber is emptied, and the device is ready for next experiment.

3 METHOD EVALUATION

The recorded data consist of five plots (T0–T4) representing the temperatures inside the sample. The temperature curves inside the sample can be divided into three characteristic phases. The first is the heating phase, during which temperature increases over time. The rate of temperature rise is highest near the hot plate and decreases with increasing distance from the heat source. Another important parameter is the time required to reach stabilization, which becomes longer for sensors located farther from the bottom. The heating rate and stabilization time can be compared between samples measured under comparable experimental conditions. However, these parameters depend not only on thermal conductivity but also on heat capacity, sensor position, and the heating conditions. Therefore, they cannot be used as independent indicators of thermal conductivity. In this study, the steady-state temperature differences are used as the primary indicators for comparing the thermal behaviour of samples with different particle sizes.
The second phase is the equilibrium phase, during which the system reaches steady state and all sensor readings remain constant. The equilibrium temperatures can be compared between samples measured under nominally identical heating conditions. However, their interpretation depends on the comparability of the heat input and heat losses. Therefore, the steady-state temperature differences between measurement positions are used for comparative evaluation, assuming sufficiently similar heat fluxes through the evaluated sections. In that case higher equilibrium temperatures suggest lower thermal conductivity. The stable temperature differences can also be used for comparison with a reference material to determine relative thermal conductivity.

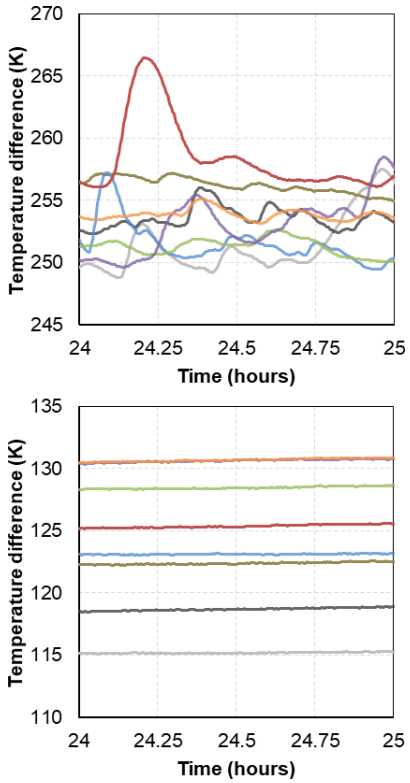


Figure 4. Zoomed in plots shown in Fig. 3; a) T0; b) T2

The final phase is the cooling phase. After the hot plate is switched off, all temperatures decrease until the sensors again reach the ambient temperature. The rate of temperature decrease, and the time required to stabilize at the final value are additional parameters that can be evaluated and compared across materials.

3.1 *Data evaluation and comparison*

The data obtained from measurements on glass beads with diameters of 1.5, 2.0, 2.5, 3.0, 3.5, 4.0, 4.5, and 5.0 mm are shown in Fig. 3. Each colour represents a different bead size, and plots corresponding to the same thermometer are grouped and labelled. The temperature curve closest to the hot plate (T0) exhibits considerable noise due to the simple two-stage regulation of the hot-plate thermostat. For this reason, the T0 curve is not suitable for quantitative analysis; however, key points such as the onset of heating, stabilization, and the end of heating can still be reliably identified. The T1 curve remains somewhat noisy as well, although the main trends are visible. Consequently, temperature differences were calculated using curves T1, T2, T3, and T4. The detail of stable parts of these plots is shown in Fig. 4.

Temperature differences for each measurement interval are listed in Tab. 1. These differences were determined at the stabilization time t = 41.6 h according to Equation (4).

$$\Delta T = \Delta T_n - \Delta T_{n+1} \tag{4}$$

Although the absolute values differ between depth intervals, the primary objective is to compare temperature differences across samples measured at the same interval. Fig. 5 presents the temperature differences for all bead sizes at all three depth intervals.

D [mm]	1.5	2.0	2.5	3.0
ΔT1-2	49.377	53.874	51.698	55.555
ΔT2-3	35.329	36.531	38.340	38.090
ΔT3-4	27.686	28.245	29.585	29.214
D [mm]	3.5	4.0	4.5	5.0
ΔT1-2	52.819	50.330	54.047	52.646
ΔT2-3	37.316	38.119	38.880	38.434
ΔT3-4	30.651	29.713	31.744	31.290

Table 1. Temperature differences $\Delta T_{1\text{-}2}$, $\Delta T_{2\text{-}3}$ and $\Delta T_{3\text{-}4}$ for various beads diameters

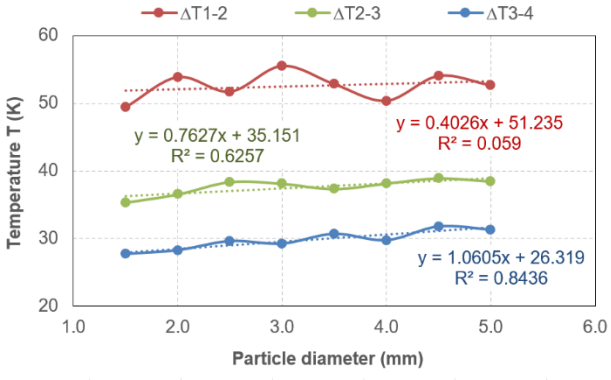


Figure 5. Temperature differences at three intervals for various beads diameters

As shown in Fig. 5, the temperature differences exhibit an overall increasing trend with increasing bead diameter, although the individual values do not increase monotonically. The scatter in the data is present and the coefficients of determination R^2 of the linear fittings are not encouraging, especially in higher temperature range.

Under the assumptions of the proposed method, the observed overall increase in temperature differences suggests a decrease in the relative effective thermal conductivity of the particulate bed with increasing bead diameter. However, due to the scatter in the data and the unverified equivalence of heat flux between experiments, this relationship should be interpreted as an observed trend rather than a definitive quantitative dependence. To evaluate this effect independently of the unknown absolute heat flux, the results were normalized according to Equation (5).

$$\lambda_n = \frac{\frac{1}{\Delta T(D)}}{\max\left(\frac{1}{\Delta T(D)}\right)} \tag{5}$$

where λn is normalised thermal conductivity and ΔT (D) is temperature differential as a function of bead diameter.

3.2 *Volumetric properties*

All samples with different bead size were also analysed regarding their volumetric properties. Volume of samples was kept uniform by filling chamber up to designated level, then the mass of every sample was measured using laboratory scale. Masses of every sample are plotted in Fig. 6a. Decrease of total mass of same volume samples with increase of bead diameter is almost linear. Total number of beads per volume unit calculated by equation (7) using known density of glass (2500 kg/m3) is decreasing following power function pictured in Fig. 6c. Bulk density was determined as follows:

$$\rho_b = \frac{m}{V_t} \tag{6}$$

where m is mass of a sample and Vt is total volume of a sample (of the chamber).

Number of beads in unit volume was determined as follows:

$$N = \frac{m}{V_t \cdot \frac{4}{3}\pi \cdot \left(\frac{D}{2}\right)^3 \cdot \rho} \tag{7}$$

where D is diameter of a glass bead and ρ is density of the glass.

Porosity was determined as follows:

$$\varepsilon = 1 - \frac{m}{\rho \cdot V_t} \quad (8)$$

Bulk density of glass beads calculated by equation (6) is lower than expected by both FCC (Face-Centered Cubic) and HCP (Hexagonal Close-Packed) packing theories, which suggest more random packing, nearing RCP (Random Close Packing) theory, that is typical for poured particulate materials (Kamien 2007).

Fig. 6 shows the volumetric properties of the samples, including sample mass, number of particles per unit volume, porosity, and bulk density for the different glass-bead sizes. The mass of the chamber fill (see Fig. 6a) decreases linearly with increasing particle diameter, from 14.50 to 13.77 kg. This trend corresponds to an increase in porosity i.e., the volume of void space within the sample filled with air which subsequently affects the heat transfer through the packed bed. Porosities of the samples, calculated using Equation (8), are shown in Fig. 6b. The values range from 0.385 to 0.416 and increase with the ball diameter. Smaller beads exhibit porosity closer to the predictions of RCP theory. The number of particles per cubic centimetre decreases following a power-law trend, ranging from 348 to 9 particles per cm³, as shown in Fig. 6c. The bulk density likewise decreases linearly, mirroring the total sample mass, from 1.54 to 1.46 g/cm³ (see Fig. 6d).

4 METHOD VALIDATION

A similar experiment was carried out on the same material samples using a TEMPOS Thermal Properties Analyzer. TEMPOS is a portable device designed to measure key thermal parameters of bulk materials (e.g., soils, concretes, insulation, and wet or frozen samples) accurately and rapidly. It employs a heated-needle (line-heat-source) probe to determine thermal conductivity, with a typical measurement time of about one minute, which helps minimize errors caused by moisture migration or free convection.

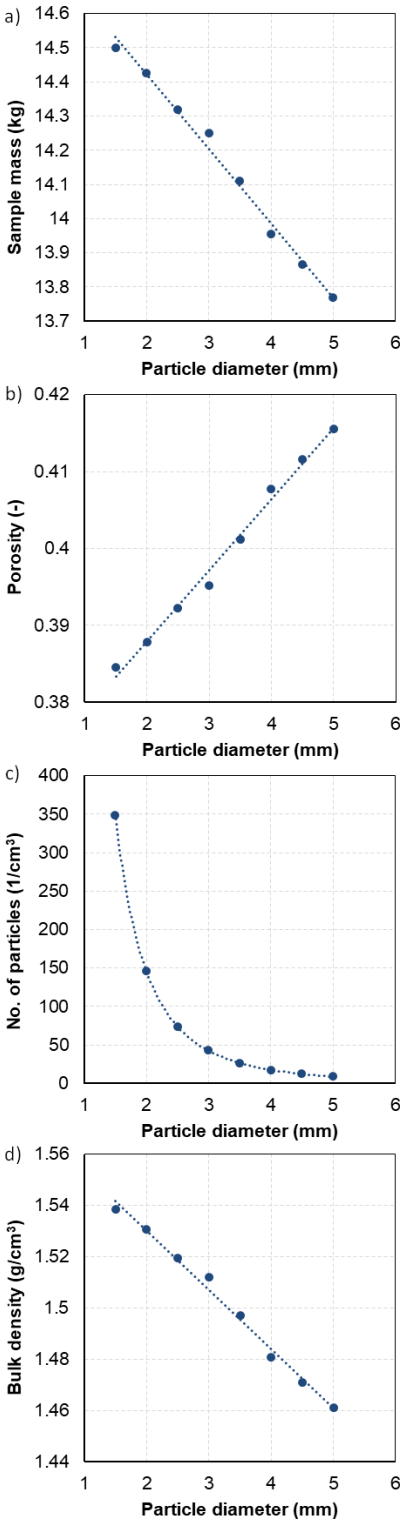


Figure 6. Volumetric properties; a) mass of a sample; b) porosity of a sample; c) No. of particles per volume unit in a sample; d) bulk density of a sample

However, the contact geometry between the needle and the sample, as well as the elimination of air gaps, is critical for obtaining reliable results. The setup of this second experiment is shown in Fig. 7a. Results of thermal conductivity using TEMPOS® analyser are shown in Fig. 7b.

The thermal conductivity measurement routine was as follows. All samples and measurement equipment were left in the same room overnight to equilibrate under identical conditions. The TEMPOS RK-3 probe was inserted into the centre of the container holding the sample and allowed to equilibrate for 15 minutes, after which the measurement was taken. Following

each measurement, the probe was removed and left to cool. The container was then closed and gently shaken. Both the sample and the probe were allowed an additional 15 minutes to dissipate the heat generated during the measurement. The probe was subsequently reinserted into the sample and left to equilibrate for another 15 minutes before the next measurement. Three consecutive measurements were performed for each sample.

The thermal conductivity values obtained for all samples are shown in Fig. 7b. A clear trend is observed: thermal conductivity decreases with increasing bead diameter. This outcome is consistent with the findings of the previous experiment.

The range of thermal conductivity between the 1.5 mm and 5 mm beads is less than 0.05 W/(m·K), which is relatively small. The sequence of values does not follow a perfectly linear trend, likely due to measurement uncertainties. This aspect warrants further investigation through repeated experiments.

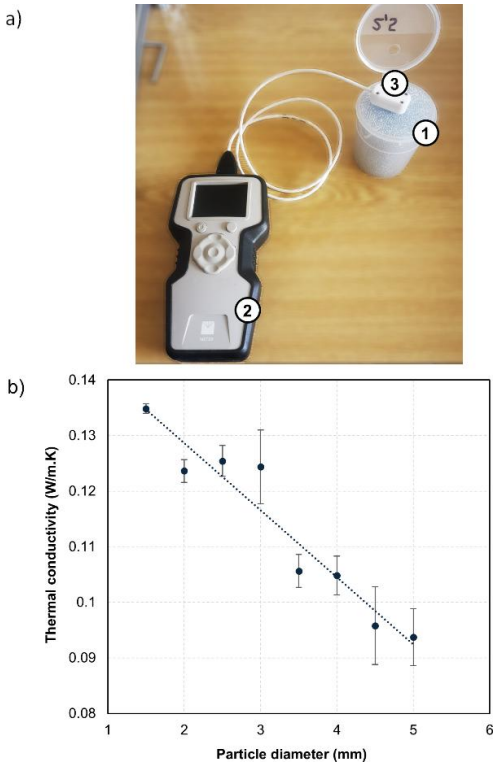


Figure 7. Validation using TEMPOS® Thermal Properties Analyzer; a) setup of the second experiment, (1) container with a sample; (2) TEMPOS® Thermal Analyzer; (3) needle probe; b) Thermal conductivity results

Although absolute thermal conductivity values are available for this experiment, comparison with the previous method requires normalization, as the aim of this article is to compare trends. Normalised values needs to be used because thermal conductivities are measured using both methods at different temperatures – thus absolute values differ as thermal conductivity is dependent on temperature itself. The dependence of normalized thermal conductivity on particle diameter is presented in Fig. 8, along with the curves from the first experiment. All plots were fitted using linear interpolation.

The results shown in Fig. 8 clearly demonstrate that the normalized thermal conductivity of the particulate bed decreases with increasing particle diameter. This trend is consistent across all measurement configurations as well as the commercial TEMPOS reference device. Linear regression analysis yielded negative slopes for all data series, confirming the inverse correlation between particle size and heat-transfer efficiency in the packed bed. The strongest dependence was observed for the TEMPOS measurements, indicating approximately a 9% decrease in normalized conductivity per millimetre increase in particle diameter. The developed device reproduced this behaviour with slightly smaller slopes, demonstrating comparable sensitivity and confirming its ability to detect particle-size-dependent variations in thermal conductivity. The smaller slopes may be attributed to radial heat losses caused by imperfect insulation of the chamber or to averaging within the measured volume.

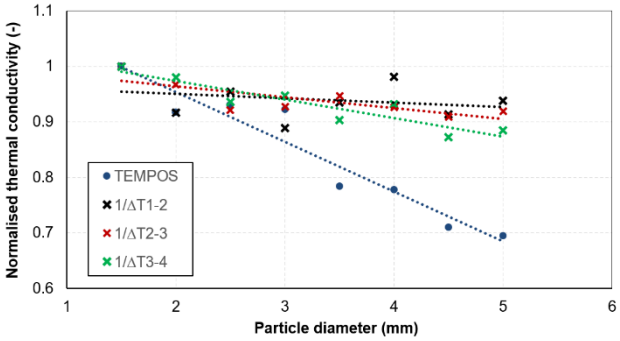


Figure 8. Normalised thermal conductivity

5 LIMITATIONS

The primary limitation of the developed method arises from the spatial averaging of temperature within the measurement chamber. Because the device records temperature gradients over a relatively large volume of particulate material, the measured values represent an averaged thermal response rather than purely one-dimensional heat conduction. This averaging effect can smooth out local variations in packing density and contact resistance, resulting in slightly reduced sensitivity to particle-size-dependent changes in thermal conductivity compared with localized probe measurements such as TEMPOS. Although the chamber was insulated with mineral wool, perfect thermal insulation could not be assumed, and radial heat losses through the side walls may have occurred during the experiments. These losses were not measured directly, as the temperature of the outer insulation surface was not monitored. Consequently, their magnitude could not be quantified from the available experimental data. The radial heat losses may have affected the heat flux through the sample and introduced additional uncertainty into the comparison of samples with different bead sizes. Therefore, the assumption of approximately equal heat flux between experiments should be regarded as an approximation rather than a verified condition. Future experiments should include monitoring of the outer insulation temperature and continuous measurement of the actual electrical power supplied to the hot plate to enable a more quantitative assessment of heat losses and heating conditions.

Therefore, while the method provides reliable trends and comparative results for coarse particulate systems, it is less suitable for precise quantification in fine powders or in materials with highly heterogeneous packing structures. The method is intended for particulate materials with particle sizes ranging from a few millimetres up to the lower tens of millimetres.

6 CONCLUSIONS

This article presents the development of an experimental method and laboratory device designed to determine the relative thermal conductivity of particulate materials. The

results indicate an overall tendency for effective thermal conductivity to decrease with increasing particle size. This trend was observed using both the newly developed device and a commercial TEMPOS analyser, although the measurements showed some scatter and the magnitude of the observed effect differed between the two methods. However, the effect observed using the developed method is much weaker than that observed using the TEMPOS analyser. This difference may be related to the higher temperature range at which the new method operates; however, this explanation has not been verified and requires further investigation. The method is particularly suited to comparative measurements of coarse granular materials ranging from a few millimetres to several tens of millimetres, whereas its applicability to fine powders is limited due to sensitivity constraints and the larger sample volume required for reliable measurements. Importantly, the device evaluates a representative bulk volume rather than relying on local probe–particle contact, making it potentially more reflective of the thermal behaviour in real industrial systems.

The outcomes of this research have potential industrial relevance in processes where heat transfer through packed beds is critical. In industries such as energy, food, pharmaceutical, chemical, metallurgical, mining, and raw-material processing, the method may support the investigation and eventual optimization of cooling, drying, and thermal-processing technologies and contribute to improving overall thermal efficiency. Beyond its practical applications, the method offers advantages in terms of simplicity, relatively straightforward operation, and cost-effectiveness, while avoiding the strict contact conditions required by many transient techniques. The method may provide comparative experimental data for future calibration of advanced numerical models such as CFD–DEM simulations. However, its repeatability and quantitative accuracy must be further evaluated before its suitability for model calibration can be established. Overall, the presented method expands the experimental toolbox for studying heat transfer in particulate systems and provides a potentially practical approach for comparative evaluation of thermal properties in granular materials. Further work is needed to quantify heat losses, assess measurement uncertainty and repeatability, and verify the method's applicability under different operating conditions.

ACKNOWLEDGMENTS

This paper was created as part of the project No. CZ.02.01.01/00/22_008/0004631 Materials and technologies for sustainable development within the Jan Amos Komensky Operational Program financed by the European Union and from the state budget of the Czech Republic, and project The European Just Transition Fund supported this work within the Operational Programme Just Transition under the aegis of the Ministry of the Environment of the Czech Republic, project CirkArena, number CZ.10.03.01/00/22_003/0000045. Work was also supported by Grant of SGS No. SP2025/005 “Development of measuring apparatus for determination of thermodynamic properties of mineral raw materials for design of process and treatment plants”, Faculty of Mining and Geology, VSB - Technical University Ostrava, Czech Republic and SGS grant no. SP2026/015, Development of laboratory equipment for the comprehensive characterization of the rheological behaviour of heavy suspensions”, Faculty of Mining and Geology, VŠB – Technical University of Ostrava, Czech Republic.

REFERENCES

[Cahill 2004] Cahill, D. Analysis of heat flow in layered structures for time-domain thermoreflectance. Review of Scientific Instruments, 2004, Vol. 75, No. 12, pp. 5119–5122. DOI: 10.1063/1.1819431.

[Cahyaningrum 2024] Cahyaningrum, F. et al. Risk management program implementation on low and medium-risk processed food manufacturers to enhance food safety control in Indonesia. IOP Conference Series: Earth and Environmental Science, 2024, Vol. 1377, No. 1. DOI: 10.1088/1755-1315/1377/1/012026.

[Carson, J 2015] Thermal conductivity measurement and prediction of particulate foods. International Journal of Food Properties, 2015, Vol. 18, No. 12, pp. 2840–2849. DOI: 10.1080/10942912.2015.1016576.

[Chalise 2023] Chalise, D. et al. High throughput, spatially resolved thermal properties measurement using attachable and reusable 3ω sensors. Review of Scientific Instruments, 2023, Vol. 94, No. 9. DOI: 10.1063/5.0151160.

[Cheng 2017] Cheng, L. et al. A small-plane heat source method for measuring the thermal conductivities of anisotropic materials. Measurement Science and Technology, 2017, Vol. 28, No. 7. DOI: 10.1088/1361-6501/aa6e81.

[Collier 2016] Collier, N. Transition and decomposition temperatures of cement phases – a collection of thermal analysis data. Ceramics-Silikaty, 2016, pp. 338–343. DOI: 10.13168/cs.2016.0050.

[Costa 2023] Costa, A. et al. Thermodynamic Modelling of Belite Clinker Mineralogy during. In: Proceedings of the 9th World Congress on Mechanical, Chemical, and Material Engineering, 2023. DOI: 10.11159/mmme23.115.

[Gu 2009] Gu, M. et al. Thermal-conductivity measurements of polymers by a modified 3ω technique. International Journal of Thermophysics, 2009, Vol. 30, No. 3. DOI: 10.1007/s10765-009-0611-5.

[Hlosta 2017] Hlosta, J. et al. Thermal Conductivity Measurement of Bulk Solids. Chemical Engineering & Technology, 2017, Vol. 40, No. 10, pp. 1876–1884. DOI: 10.1002/ceat.201700018.

[Hlosta 2018a] Hlosta, J. et al. Analysis and Optimization of Material Flow inside the System of Rotary Coolers and Intake Pipeline via Discrete Element Method Modelling. Energies, 2018, Vol. 11, No. 7. DOI: 10.3390/en11071849.

[Hlosta 2018b] Hlosta, J. et al. CFD-DEM numerical model of laboratory scale fluidized bed coffee roaster. In: ICNAAM 2018 – 16th International Conference of Numerical Analysis and Applied Mathematics, 13–18 September 2018.

[Kamien 2007] Kamien, R. and Liu, A. Why is Random Close Packing Reproducible? Physical Review Letters,

2007, Vol. 99, No. 15. DOI: 10.1103/PhysRevLett.99.155501.

[Lee 2006] Lee, J. et al. Thermal and electrical conductivities of porous carbon-coated ceramic fiber composites. Key Engineering Materials, 2006, Vol. 317–318, pp. 491–494. DOI: 10.4028/www.scientific.net/KEM.317-318.491.

[Liu 2014] Liu, Z. et al. Recursive singular value decomposition based parameter estimation for thermal efficiency on-line monitoring of the cement clinker manufacturing process. In: Proceedings of the 11th World Congress on Intelligent Control and Automation, 2014, pp. 2780–2785. DOI: 10.1109/WCICA.2014.7053167.

[Mirkovic-Marjanovic 2022] Mirkovic-Marjanovic, M. et al. Verification and validation of an advanced guarded hot plate for determination of thermal conductivity. Thermal Science, 2022, Vol. 26, No. 6A, pp. 4735–4747. DOI: 10.2298/TSCI220311108M.

[Moses 2023] Moses, I. Review on thermal energy audit of pyro-processing unit of a cement plant. International Journal of Energy and Environmental Research, 2023, Vol. 11, No. 1, pp. 54–74. DOI: 10.37745/IJEER.13/VOL11N15474.

[Oyepata 2021] Oyepata, J. et al. Modelling of clinker cooler and evaluation of its performance in clinker cooling process for cement plants. Nigerian Journal of Technology, 2021, Vol. 39, No. 4, pp. 1093–1099. DOI: 10.4314/njt.v39i4.16.

[Park 2023] Park, J. Development of briquetting technology for fine ore agglomeration in sintering process. In: Proceedings of the 9th World Congress on Mechanical, Chemical, and Material Engineering, 2023. DOI: 10.11159/mmme23.104.

[Salim 2022] Salim, S. Thermal conductivity measurements using the transient hot-wire method: a review. Measurement Science and Technology, 2022, Vol. 33, No. 12. DOI: 10.1088/1361-6501/ac90df.

[Shapiro 2004] Shapiro, M. et al. Characterization of Powder Beds by Thermal Conductivity: Effect of Gas Pressure on the Thermal Resistance of Particle Contact Points. Particle & Particle Systems Characterization, 2004, Vol. 21, No. 4, pp. 268–275. DOI: 10.1002/ppsc.200400943.

[Stepanic 2019] Stepanic, N. et al. An in situ temperature calibration of a guarded hot plate apparatus. Thermal Science, 2019, Vol. 23, No. 2A, pp. 707–715. DOI: 10.2298/TSCI180425176S.

[Verma 2020] Verma, Y. et al. Thermal energy consumption and its conservation for a cement production unit. Environmental Engineering Research, 2020. DOI: 10.4491/eer.2020.111.

CONTACTS:

Ing. Jakub Hlosta Ph.D.
VSB-Technical University of Ostrava
Faculty of Mining and Geology
17. listopadu 15/2172, 708 00, Ostrava-Poruba, Czech Republic
jakub.hlosta@vsb.cz

LICENSE CREATIVE COMMONS:

The article is published under the terms and conditions of the Creative Commons Attribution 4.0 International License (CC BY 4.0).